Journal of Cellular Biochemistry 45:93–100 (1991)

Cell Density-Dependent Decrease in Cytoskeletal Actin and Myosin in Cultured Osteoblastic Cells: Correlation With Cyclic AMP Changes

John J. Egan, Gloria Gronowicz, and Gideon A. Rodan

Laboratory of Cellular and Developmental Biology, National Institute of Diabetes, Digestive and Kidney Diseases, National Institutes of Health, Bethesda, Maryland 20892 (J.J.E.); Department of Orthopedic Surgery, The University of Connecticut Health Center, School of Medicine, Farmington, Connecticut 06032 (G.G.); Department of Bone Biology and Osteoporosis Research, Merck Sharp & Dohme Research Laboratories, West Point, Pennsylvania 19486 (G.A.R.)

Abstract During bone development, osteoblasts form a contiguous layer along recently deposited osteoid and their morphology changes from fibroblast-like to cuboidal. In culture, similar changes occur with increased cell density. We examined the possible role of cyclic AMP in this process since cyclic AMP was reported to increase in fibroblasts with increased cell density and similar shape changes were seen in response to parathyroid hormone, which also increases cellular cyclic AMP in osteoblastic cells. Osteoblast-enriched rat calvaria cells were seeded at increasing density. The distribution between Triton X-100 extractable and nonextractable actin and myosin was estimated by polyacrylamide gel electrophoresis. Intracellular cyclic AMP was estimated by prelabeling the cellular ATP pool with ^{3}H-adenine, followed by extraction and separation of ^{3}H-cAMP by high-performance liquid chromatography. We found that osteoblastic cells contain about 40 pg actin and 5.3 pg myosin per cell. Around 60% of the actin and 70% of the myosin were in the nonextractable (crosslinked) form at cell densities of 10,000 to 50,000 cells per cm^2. Above 50,000 cells/cm^2, there was a cell density-dependent reduction in crosslinked actin and myosin and a concomitant increase in cellular cyclic AMP. A comparable rise in cyclic AMP, produced by incubation with phosphodiesterase inhibitors, and treatment with other agents that increase cyclic AMP produced a similar decrease in the level of cytoskeletal actin and myosin. Cytochalasin B treatment, through its effect on actin polymerization, produced similar changes in cell shape and cytoskeletal actin. The findings suggest that an elevation in intracellular cyclic AMP may play a role in the density-dependent changes in cell shape and microfilament organization observed in osteoblasts.

Key words: cytoskeleton, osteoblasts, cell-cell interaction

In several mesenchyme-derived cells, including adipocytes [1], chondrocytes [2], and synovial cells [3], cell shape influences gene expression and differentiation. Osteoblasts are found on advancing surfaces of developing bones. During differentiation, they form a contiguous layer of cells and assume a "cuboidal" morphology. In addition, osteoblasts are polarized toward the underlying bone surface and secrete numerous bone matrix proteins at the mineralizing front. The process by which osteoblasts and other cells maintain their characteristic shape and organization is probably important for their function. The shape of mesenchymal cells in monolayer cultures is also dependent on cell density: At low density, they are elongated and have multiple processes, whereas at high density, they appear more rounded with fewer cell processes [4]. The biochemical pathways responsible for the density-related shape changes are not fully known. It was reported that in C3H 10 T-½ cells [5] and in synovial fibroblasts [6] microfilament polymerization decreases with cell density. In fibroblasts, it has been shown that cyclic AMP levels increase with cell density [7,8]. In osteoblastic cells, parathyroid hormone stimulates cyclic AMP accumulation and produces similar shape changes, along with a reduction in cytoskeletal actin and myosin [9]. In smooth muscle [10], cyclic AMP (cAMP) causes depolymerization of microfilaments through a mechanism that was proposed to involve regulation of myosin light chain kinase activity. The objective of this study was to examine if the change in cell density-

Received June 7, 1990; accepted October 3, 1990.

dependent shape was accompanied by changes in cytoskeletal actin and myosin and if these correlated with changes in cAMP. We found that starting at about 50,000 cells/cm^2, there is a density-dependent decrease in cytoskeletal actin and myosin per cell and a concurrent increase in cAMP. Other agents that increase cAMP levels produced similar changes in cytoskeletal proteins.

MATERIALS AND METHODS

Materials

Collagenase (Type I), hyaluronidase (Type I), Trypsin (Type III), cytochalasin B, purified rabbit muscle actin and myosin, and all other reagents were obtained from Sigma Chemical Co., St. Louis, MO; Nunclon 4-well tissue culture dishes were from Nunc, Roskilde, Denmark; tissue culture dishes (100 × 20 mm; 60 × 15 mm; 35 mm, 6-well clusters) were from Costar, Cambridge, MA; F-12 medium, horse serum, and Kanamycin sulfate were from GIBCO, Grand Island, NY; fetal bovine serum was from KC Biological, Lanexa, KA; and pregnant Sprague-Dawley rats were from Charles River Farms, Wilmington, MA. Antibodies to myosin heavy chain were the generous gift of Dr. James R. Sellars (NHLBI, NIH). The antibody to actin was from Biomedical Technologies Inc. Phosphodiesterase was a gift from Dr. Paul M. Epstein, Department of Pharmacology, University of Connecticut. 1–34 Parathyroid hormone peptide (human sequence) was from Bachem Corp., Torrance, CA; forskolin was from Calbiochem-Behring Corp., La Jolla, CA.

Methods

Isolation and cell culture of fetal rat calvaria osteoblasts. Primary cultures of fetal rat calvaria cells were obtained by digestion in 2% collagenase and 1% hyaluronidase. The third digest yielded osteoblast-enriched cells (typically 6 × 10^6 per 30 calvaria) [11]. Cells were washed and cultured to confluence (230,000 cells/cm^2; 9–10 days) in medium containing 5% horse serum, 2% fetal bovine serum, and 1% Kanamycin sulfate in modified F-12 [12]. Culture medium was changed every 4 days.

For all experiments, secondary cultures were used at the cell densities indicated. Cells were dispersed with freshly thawed trypsin, (0.01% in calcium, magnesium-free Hank's balanced salt solution, CMFH), washed with culture medium, and plated into NUNC 4-well dishes (2 cm^2 surface area) to yield the desired densities between 20,000 and 100,000 cells/cm^2. Cell counts at 12 and 24 h after plating showed no increase in cell number during this period. The plating efficiency was around 80% (Table I). Actual cell density was determined at the time of the experiment 24 h after plating by counting trypsin-dispersed cells with a Coulter counter on four independent parallel culture wells from the same experiment. The coefficient of variation for cell counts between culture wells was 5%.

In one series of experiments, the volume of the culture media was adjusted to the number of cells plated, to exclude differences in "conditioning" of the media as a possible reason for the density-dependent changes. These experiments yielded the same results, as reported below.

TABLE I. Effect of Increasing Cell Density on the Distribution of Actin and Myosin Between the Triton-Insoluble and Soluble Fractions in Rat Osteoblastic Cells

Plated	Attached cells/cm^2	Plating efficiency	Actin (pg/cell)		Myosin (pg/cell)	
			Insoluble	Soluble	Insoluble	Soluble
20,000	18,750	93	22 ± 0.3	15 ± 0.4	3.8 ± 0.3	1.5 ± 0.2
40,000	30,000	75	24 ± 0.2	16 ± 0.7	3.7 ± 0.4	1.5 ± 0.1
60,000	50,319	84	21 ± 0.2	18 ± 0.5	3.8 ± 0.6	1.4 ± 0.3
80,000	65,625	82	16 ± 0.4	22 ± 0.7	3.1 ± 0.3	2.2 ± 0.3
100,000	81,250	81	12 ± 2.0	26 ± 1.0	2.0 ± 0.5	3.3 ± 0.2
125,000	93,159	75	10 ± 0.8	27 ± 1.2	1.6 ± 0.3	3.6 ± 0.3

Rat calvaria osteoblasts obtained as described in Materials and Methods were plated in secondary cultures. The number of cells/cm^2 added to each well (2 cm^2) is shown in the first column and the number of attached cells in the second. The amount of insoluble and soluble actin and myosin were estimated on triplicate wells as described in Methods. This is one of three similar experiments.

Separation of triton X-100-soluble and -insoluble proteins. At 24 ± 2 h after seeding, following a gentle wash with 0.5 ml of CMFH (pH 7.7 at 37°C), cells from each density were exposed for 10 min at 4°C (ice bath) to 0.1 ml of ice-cold 1% Triton X-100 extraction medium [13], (1% [w/v] Triton X-100, 40 mM KCl, 10 mM Imidazole, pH 7.0, 10 mM EGTA, and 0.5 mM EDTA). The extraction was repeated twice, and the combined samples were centrifuged (14,000*g* for 4 min). This procedure yielded a Triton-insoluble pellet that was washed again. The Triton-soluble fraction and -insoluble pellet were run on SDS, 5–15% polyacrylamide gel electrophoresis [14].

Gels were stained with 0.2% Coomassie Brilliant Blue R-250, and the protein bands were scanned for absorbance. The mass of actin and myosin was determined from standard curves obtained by scanning the absorbance of purified actin and myosin standards processed at the same time (Fig. 4b). Absorbance was linear between 0.1 and 5.0 μg for both proteins as reported elsewhere [15]. The data obtained as μg protein per well was expressed as pg/cell using the cell counts determined in parallel wells.

Identification of actin, myosin heavy chain and myosin light chain by Western blot analysis. Cells were plated into secondary culture in 35 mm diameter (6-well cluster) dishes, and the cell density, estimated with a Coulter counter in parallel wells 24 h after plating, was 35,000 cells/cm^2. Cells were treated with 1% ice-cold Triton X-100 extraction medium and separated into Triton-soluble and -insoluble fractions as described above. Protein samples were processed on 10% acrylamide SDS-PAGE. The wet gels were electroblotted onto nitrocellulose overnight at 50 V, 4°C. The blots were incubated with antibody to myosin heavy chain (1:50 dilution) and to actin (1:100 dilution). The presence of immunoreactive antibody was visualized in autoradiographs of Western blots that were incubated with ^{125}I-protein A.

Measurement of steady-state levels of cAMP. The ATP pool was labeled to constant specific activity with 5 μCi/ml [^{3}H]-adenine for 2 h at 37°C [16,17]. The cells were washed with 5 ml CMFH (37°C); ATP and cAMP were extracted by exposure to 10% TCA for 30 min at 23°C. The extract was transferred to polypropylene tubes and exogenous cAMP (5 nmoles) was added as carrier. Samples were frozen, thawed, centrifuged (3000 RPM/30 min) to precipitate protein and warmed to 30°C to solubilize cAMP, and the supernatant was neutralized with 10 μl of 4 N KOH.

The [^{3}H]-adenine nucleotides were separated on C_{18} ion-pair reverse phase HPLC (300 mm × 3.9 mm I.D.) at 2 ml/min with mobile phase: 65 mM KH_2PO_4, pH 3.6, 2% acetonitrile, 1.5 mM tetrabutylammoniumphosphate [18]. The retention time of ATP was 10–11 min, and of cAMP, 23 min. Samples were collected and counted by liquid scintillimetry. Authenticity of cyclic AMP was determined following treatment of [^{3}H]-cyclic AMP (separated above) with phosphodiesterase and rechromatography, wherein disappearance of greater than 95% radioactivity was observed.

Calculations for steady-state levels of cyclic AMP were based on cpm [^{3}H]-cyclic AMP eluted above and on the specific radioactivity of ATP in the same sample. Areas of absorbance for ATP (254 nM) were integrated, and the moles were calculated from a standard curve established by chromatography of ATP (Sigma, A-2383) dissolved in extraction medium and separated as above. Values for cyclic AMP are expressed in fmole/cell.

RESULTS

Effect of Cell Density on the Mass of Triton-insoluble Actin and Myosin

The morphological appearance of cells seeded at increasing density is shown in Figure 1. At 35,000 cells/cm^2, the cells are elongated with many long projections that extend to neighboring cells. With increasing density, starting at around 50,000 cells/cm^2, many cells appear more rounded or cuboidal and have fewer projections.

Figure 2 shows the polyacrylamide gel profiles of the Triton-soluble (lane a) and cytoskeletal fractions (lane b). Two-dimensional gel electrophoresis (data not shown) indicated that actin and myosin are the major bands migrating at 42 KD and 200 KD, respectively.

The identity of actin and myosin heavy chains was corroborated by Western blot analysis (Fig. 3). The mass of actin and myosin was determined from one-dimensional gels as described in Methods, using the calibration curves, presented in Figure 4b, which were run with each experiment. The combined recovery of actin and

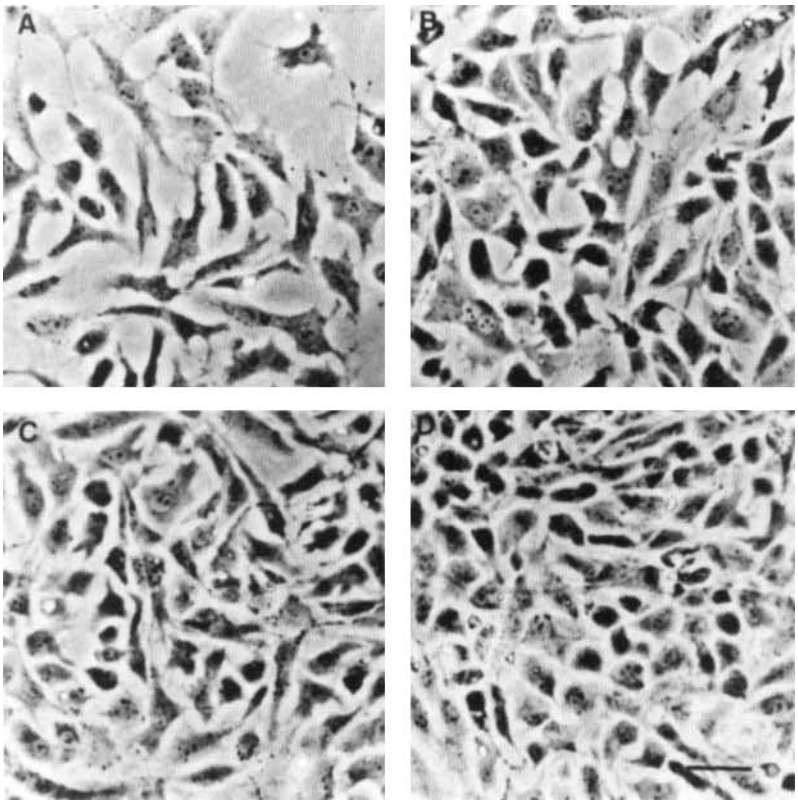

Fig. 1. Phase contrast microscopy of cells plated at increasing cell density. Cells were plated into 35 mm diameter tissue culture dishes to yield the following cell densities, determined 24 h after plating: **A:** 35,000/cm^2; **B:** 58,000/cm^2; **C:** 80,000/cm^2; **D:** 120,000/cm^2.

myosin in the two fractions was very similar in all experiments (Table I).

Figure 4a shows the distribution of myosin and actin between the Triton-soluble and -insoluble compartments in cells seeded at 50,000 cells/cm^2. The mean mass of Triton X-100 insoluble actin was 23.0 ± 1.2 pg/cell, and myosin, 3.6 ± 0.6 pg/cell (SEM, 30 experiments). Under these conditions, about 60% of the cellular actin and 70% of the cellular myosin are found in the Triton-insoluble fraction. The same distribution between the Triton-insoluble and soluble forms was seen at cell densities up to 50,000 cells/cm^2 (Table I; Fig. 5). However, at 65,000 cells/cm^2, there was a 30%, statistically significant, reduction in the amount of Triton-insoluble actin, and at 80,000 cells/cm^2, there was a 50% reduction in Triton-insoluble actin and myosin, without changes in total cell actin and myosin.

Effect of Cell Density on Steady State Levels of cAMP

The mean steady-state level of cAMP in cells seeded below 50,000 cells/cm^2 was 0.23 fmoles/cell (Fig. 5). Above this cell density, there was a linear increase in cAMP content up to 0.4 fmole/cell at 80,000 cells/cm^2. Concomitant with the assessment of cAMP levels at various cell densities, the amount of actin and myosin associated with the Triton-insoluble and -soluble fractions was determined as described above. A close inverse relationship was found between cAMP content and cytoskeleton-associated actin and myosin above 50,000 cells/cm^2 ($r = 0.95$).

Effect of cAMP-Elevating Agents on Cytoskeletal Actin and Myosin

The exposure of cells to agents that increase cAMP levels: forskolin (FSK, 10 μM), isobutylmethylxanthine (IBMX, 200 μM), papaverine (200 μM), and 8Br cAMP (0.5 mM), decreased Triton-insoluble actin and myosin to the same extent as did 0.1 μM PTH (1-34) (Fig. 6). Cellular cAMP levels, estimated as described in Methods, were raised at 5 min to 0.35 ± 0.04 fmoles/cell by IBMX, 5.5 ± 0.14 by PTH, and 9.2 ± 0.65 by FSK, compared to 0.17 ± 0.03 for vehicle-treated cells.

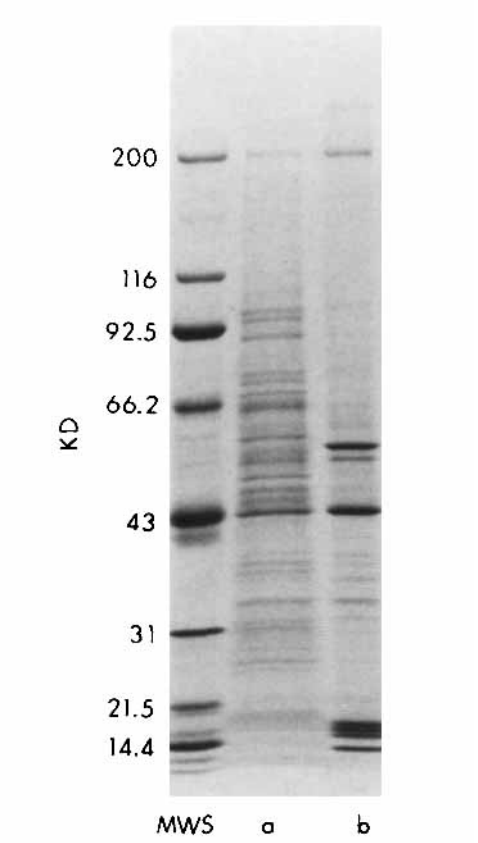

Fig. 2. SDS-PAGE electrophoresis of Triton-soluble and -insoluble (cytoskeletal) proteins. Cells were plated at 50,000 cells/cm^2, and 24 h later, the Triton-soluble (**lane a**) and -insoluble (cytoskeletal) fractions (**lane b**) were analyzed by SDS-PAGE as described in Methods. MWS corresponds to the molecular weight standards, denoted along the left margin, in kilodaltons.

Effect of Cytochalasin B on Cytoskeletal Actin and Myosin

To determine if agents that are known to disrupt the cytoskeleton would also alter the Triton-insoluble cytoskeleton pellet, cytochalasin B was added to the osteoblast culture. The effect of 12 μM cytochalasin B on cytoskeletal actin and myosin mimicked those of cAMP-elevating agents and produced approximately the same effect as did 100 nM PTH (Table II). Moreover, the effects of cytochalasin B and PTH were non-additive, suggesting that a common microfilament pool was the target for both agents.

DISCUSSION

In several systems it was shown that the Triton X-100 insoluble proteins are components of the cytoskeleton [19,20]. This observation serves as the operational definition for cytoskeletal actin and myosin in this study. While F-actin itself is quantitatively precipitated at high centrifugal forces (100,000*g* for 3 h), in the presence of 1 mM Mg^{2+} [21], the low-speed centrifugation used here should only precipitate polymeric cytoskeletal actin. To prevent actin and myosin degradation by Ca^{2+}-dependent proteases, EGTA was present in the extraction medium [13]. Using this method and a calibration procedure, we obtained highly reproducible estimates of cellular actin and myosin. The amount of actin in osteoblastic cells was consistent with that observed in many other cell types [5]. The

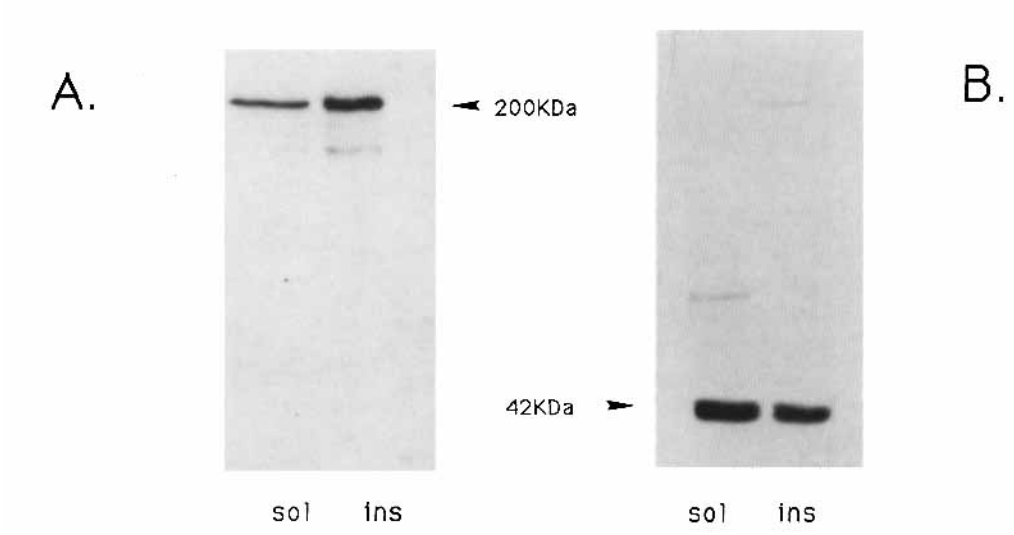

Fig. 3. Identification of myosin heavy chain and actin in osteoblastic cells by specific antibodies. Cells were cultured, and cytoskeletal proteins were extracted and chromatographed as described in Methods. Western blot analysis of myosin heavy chain is shown in autoradiogram, **panel A,** and actin in autoradiogram, **panel B.**

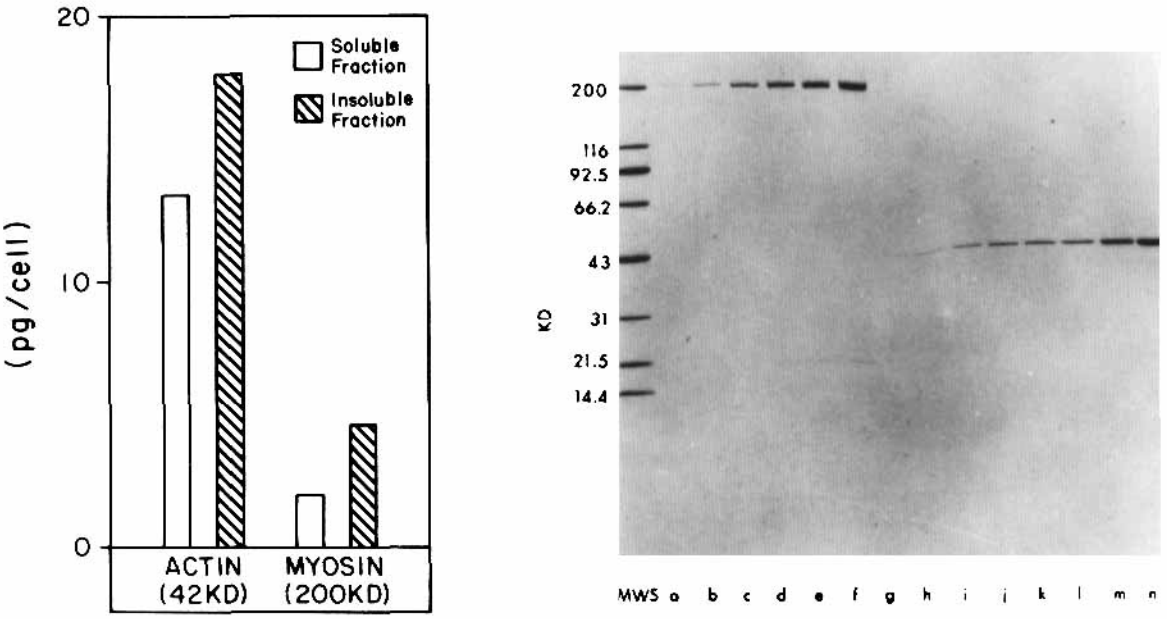

Fig. 4. Distribution of actin and myosin between the Triton-soluble and -insoluble (cytoskeletal) fractions in resting osteoblast. **a:** The mass of actin and myosin in the Triton-soluble (open bars) and -insoluble (hatched bars) fractions was determined as described in Methods. **b:** SDS-PAGE gels of purified myosin and actin standards were prepared and stained with Coomassie Blue as described in Methods, and the bands were scanned for absorbance. MWS, molecular weight standards. Myosin, **lanes a–f:** a, 0.217 μg; b, 0.435 μg; c, 0.870 μg; d, 1.304 μg; e, 1.739 μg; f, 2.174 μg. Actin, **lanes g–n:** g, 0.1 μg; h, 0.2 μg; i, 0.4 μg; j, 0.6 μg; k, 0.8 μg; l, 1.0 μg; m, 2.0 μg; n, 4.0 μg.

content of cytoskeletal actin and myosin was similar to that observed in leukocytes [15]. The distribution of actin between the Triton-soluble and -insoluble fractions (60/40) is similar to that reported in NRK cells [22] and in C3H 10 T-½ cells [5]. The distribution of myosin between the two fractions has not been studied in many systems, but its similarity to that of actin suggests that the two may be functionally related. This idea is supported by the co-localization of

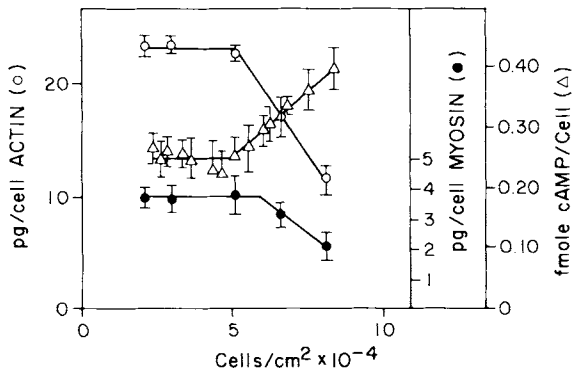

Fig. 5. The effect of cell density on the mass of cytoskeletal actin and myosin and on the steady-state levels of cAMP in osteoblastic cells. Twenty-four hours after plating, cells were extracted with Triton X-100, and the mass of actin (open circles) and myosin (closed circles) in the cytoskeletal fraction was determined as described in Methods. In parallel wells of the same experiments, cells were labeled with 5 μCi/ml [^{3}H]-adenine for 2 h, after which the medium was removed, the cells were washed, lysed, and prepared for HPLC to separate [^{3}H]-cAMP and [^{3}H]-ATP and to estimate cAMP levels (open triangles) as described in Methods. Data represent mean ± SEM from three separate experiments.

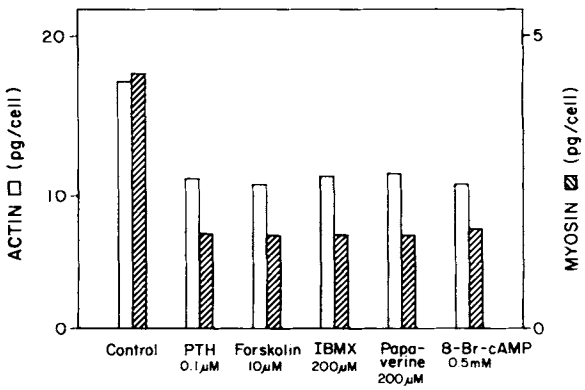

Fig. 6. The effect of cAMP-elevating agents on the mass of cytoskeletal actin and myosin. Cells were plated into Nunc dishes between 40,000–60,000 cells/cm^2. Twenty-four hours later, cells were washed and treated with various agents at the indicated concentrations for 5 min at 37°C, and the Triton-insoluble proteins were processed as described in Methods. Open bars represent the mass of Triton-insoluble actin, and hatched bars, the mass of Triton-insoluble myosin, both expressed as pg/cell.

TABLE II. Effect of Cytochalasin B on Cytoskeletal Actin in Osteoblastic Cells

Condition	Actin (pg/cell)
Control	18.6 ± 1.39[a]
DMSO (0.01%)	20.2 ± 1.43
Cytochalasin B	
(0.12 μM)	16.2 ± 1.02
(1.2 μM)	13.8 ± 1.37
(12.0 μM)	12.0 ± 1.28

Cells were plated into Nunc dishes at 55,000 cells/cm^2. Twenty-four hours later, the cells were treated with cytochalasin B or vehicle (DMSO) at the concentrations indicated for 30 min. The cytoskeleton proteins were separated and processed as described in Methods. "Control" represents a 30 min time point in the absence of vehicle. Data are expressed as mean ± SEM of quadruplicate determinations from one of two similar experiments.

myosin filaments with actin-containing microfilaments [23,24].

When cells were seeded at increasing density, they assumed a more cuboidal appearance above approximately 50,000 cells/cm^2. The fraction of cytoskeletal actin and myosin remained constant up to that density, but decreased significantly thereafter, reaching half the initial level at 80,000 cells/cm^2. A similar observation was made with respect to actin in NRK cells, where the F-actin was quantitated by SDS-PAGE [22] and in C3H 10 T-½ cells where F-actin was estimated indirectly from DNase I inhibition assays [5]. The mass of cytoskeletal myosin was not estimated in those studies. The parallel changes in actin and myosin observed here suggest that the alteration occurs in actin filaments associated with myosin. The above findings show that in elongated cells, with numerous cell processes, a high fraction (60%) of the actin and myosin is present in the Triton non-extractable form and that this fraction decreases to about half (30%) when cells are more closely packed and assume a more rounded morphology. Although similar morphological states exist in vivo, it remains to be shown if the observations made in cell culture apply to in vivo conditions. Both in vivo and *in culture* differentiation in several systems was shown to coincide with cellular condensation and changes in cell shape, but the molecular linkage between cell contacts, cell shape, cytoskeletal changes, and gene expression remain to be elucidated.

The signals responsible for the reduction in cytoskeletal actin and myosin, with increased cell density in the experiments described here, are also not known. However, the findings suggest that cAMP may play a regulatory role in this phenomenon. We confirmed previous observations showing cell density-dependent increases in cAMP [7,8] and showed a tight inverse correlation between the rise in cAMP and the reduction in cytoskeletal actin and myosin. Moreover, all agents that increase cAMP had similar effects. The elevation of cAMP, produced by cell density, was modest compared to that produced by hormonal stimulation. However, cells exposed to the phosphodiesterase inhibitor IBMX, which increased cAMP content to about the same extent as high cell density, showed a similar decrease of about 50% in cytoskeletal-associated actin and myosin. Interestingly, the much higher increase in cAMP levels produced by forskolin or parathyroid hormone did not cause further reduction in the actin and myosin content of the Triton-insoluble fraction, suggesting that only a fraction of the total cytoskeletal actin and myosin may be susceptible to this regulation. It is not surprising that very small changes in cellular cyclic AMP suffice to produce the maximum biological effect since very small changes in cAMP were shown to fully activate the cAMP-dependent protein kinase in these [25] and other cells. The effects of phosphodiesterase inhibitors, parathyroid hormone, and forskolin on cAMP levels on one hand and on the cytoskeletal proteins on the other hand are fully consistent with this view.

The pathway for the regulation of actin and myosin polymerization by cAMP in this system is not known. In smooth muscle, cAMP-induced actomyosin depolymerization was proposed to result from inactivation of myosin light chain kinase caused by cAMP-dependent phosphorylation, which, in turn, leads to reduced phosphorylation of the myosin light chain [26]. Other possibilities include the phosphorylation of myosin heavy chain, which was observed in myeloid leukemia cells [27] and *Dictyostelium* [24], macrophages [28], and BHK cells [29] and was shown to inhibit myosin polymerization in *Acanthamoeba* [30]. Still another possibility is the activation of a putative myosin light chain phosphatase about which little is known.

In summary, the findings presented here show an inverse correlation between cell density-dependent increases in cyclic AMP and decreases in cytoskeletal actin and myosin, suggesting a functional relationship between these

changes and a close association between the two proteins.

REFERENCES

Spiegelman BM, Ginty CA: Cell 35:657–666, 1983.

Benya PD, Shaffer JD: Cell 30:215–224, 1982.

Aggeler J, Frisch SM, Werb Z: J Cell Biol 98:1662–1671, 1984.

Otten J, Johnson GS, Pastan I: J Biol Chem 247:7082–7087, 1972.

Heacock CS, Eidsvoog KE, Bamburg JR: Exp Cell Res 153: 402–412, 1984.

Unemori EN, Werb Z: J Cell Biol 103:1021–1031, 1986.

Sheppard JR: Nature (New Biol) 236:14–16, 1972.

Anderson WB, Pastan I: Adv Cyclic Nucleotide Res 5:681–698, 1975.

Egan JJ, Gronowicz G, Rodan GA: Submitted.

Adelstein RS, Conti MA, Hathaway DA, Klee CB: J Biol Chem 253:8347–8350, 1978.

Wong GL: J Biol Chem 254:6337–6340, 1979.

Majeska RJ, Nair BC, Rodan GA: Endocrinology 116:170–179, 1985.

Rosenberg S, Stracher A, Lucas R: J Cell Biol 91:201–211, 1981.

Laemmli UK: Nature 227:680–685, 1970.

White JR, Naccache PH, Sha'afi RI: J Biol Chem 258:14041–14047, 1983.

Rodan SB, Insogna KL, Vigerny AMC, Stewart AF, Broadus AE, D'Souza SM, Bertolini DR, Mundy GR, Rodan GA: J Clin Invest 72:1511–1515, 1983.

Humes JL, Rounbehler M, Kuehl F, Jr: Anal Biochem 32:210–217, 1969.

Jahngen EGE, Rossomando EF: Anal Biochem 173:493–504, 1984.

Gonella PA, Nachmias VT: J Cell Biol 89:146–151, 1981.

Jennings LK, Fox JEB, Edward HH, Phillips DR: J Biol Chem 256:6927–6932, 1981.

Korn ED: Physiol Rev 62:672–737, 1982.

Rubin RW, Warren RH, Kukeman DS, Clements E: J Cell Biol 78:28–35, 1978.

Lazarides E: Methods Cell Biol 24:313–331, 1982.

Yumura S, Fukui Y: Nature 314:194–196, 1985.

Partridge NC, Kemp BE, Veroni MC, Martin TJ: Endocrinology 108:220–225, 1981.

DeLanerolle P, Nishikawa M, Yost DA, Adelstein RS: Science 223:1415–1417, 1984.

Sagara J, Nagata K, Ichikawa Y: Biochem J 214:839–843, 1983.

Trotter JA, Nixon CS, Johnson MA: J Biol Chem 260:14374–14378, 1985.

Kuczmarski ER: J Cell Biol 97:264a, 1983.

Kuznicki J, Albanesi JP, Cote GP, Korn ED: J Biol Chem 258:6011–6014, 1983.